CHAPTER 2: VALIDATION OF THE SUPERPAVE BINDER PARAMETER FOR RUTTING BASED ON ALF PAVEMENT TESTS AT 58 °C

1. Superpave Binder Parameter for Rutting

a. Derivation of G*/sinδ

The Superpave binder specification uses the parameter G*/sinδ to specify binders according to rutting susceptibility at high pavement temperatures. This parameter is measured using a dynamic shear rheometer (DSR), which subjects a sample of binder between two parallel plates to oscillatory shear. Tests in this study were performed on RTFO residues. The high-temperature continuous PG of each binder is the temperature that provides a G*/sinδ of 2.20 kPa.

The binder specification also requires unaged binders to be tested by the DSR at high temperatures to control tenderness. To accomplish this, the temperature that provides a G*/sinδ of 1.00 kPa is determined. These temperatures were obtained, but they were not used in this study. Table 2 in chapter 1 shows that the two sets of high-temperature grades were close.

The binder parameter G*/sinδ is based on dissipated energy. With each cycle of loading, the work done in deforming an asphalt or an asphalt pavement at high temperatures is partially recovered by the elastic component of the strain and partially dissipated by the viscous flow component of the strain and any associated generation of heat. The energy dissipated by the viscous flow component per cycle of loading can be calculated using:

$$\Delta U = \int \tau \, d\gamma \tag{1}$$

The following relationship is obtained for a sine wave loading upon integrating equation (1) from 0 to 2π:[13]

$$\Delta U = \pi \, \tau_{max} \, \gamma_{max} \, \sin\delta \tag{2}$$

where:
- ΔU = Energy loss per cycle, or dissipated energy
- π = 3.14159,
- τ = Shear stress,
- γ = Shear strain,
- τ_{max} = Maximum shear stress,
- γ_{max} = Maximum shear strain, and
- δ = Phase angle.

Superpave uses a stress-controlled type of pavement loading where each binder will be subjected to the same maximum stress or set of stresses. Therefore, the maximum shear stress is a constant along with π, and equation (2) becomes:

$$\Delta U \propto \gamma_{max} \sin\delta \quad (3)$$

Since $|G^*| = \tau_{max}/\gamma_{max}$ and $\gamma_{max} = \tau_{max}/|G^*|$, equation (2) can also be written as follows:

$$\Delta U = (\pi \tau_{max}^2 \sin\delta)/|G^*| \quad (4)$$

where: $|G^*|$ = the absolute value of the complex shear modulus.

For a stress-controlled type of pavement loading, the maximum shear stress is a constant along with π, and thus equation (4) becomes:

$$\Delta U \propto \sin\delta/|G^*| \quad (5)$$

Superpave uses this equation because $|G^*|$ is a constant in the linear viscoelastic range. Therefore, all asphalt binders do not have to be tested using the same maximum shear stress. Furthermore, a stress- or strain-controlled DSR can be used to obtain the individual parameters G* and $\sin\delta$. These parameters can then be used to calculate $\sin\delta/|G^*|$, which is only valid for a stress-controlled mode of loading applied in the form of a sine wave in the linear viscoelastic range.

As $\sin\delta/|G^*|$ decreases, rutting susceptibility should decrease. This can be accomplished by decreasing $\sin\delta$ or increasing $|G^*|$. $|G^*|$ is a measure of the total resistance of the binder to strain. $\sin\delta$, which is equal to the loss modulus G" divided by G*, is a relative measure of the viscous flow component of the strain. Equations (3) and (5) are equivalent, but the meaning of ΔU is more readily apparent using equation (3). In equation (3), dissipated energy is proportional to the permanent shear strain, which is the maximum shear strain times $\sin\delta$. Thus, if the response to a stress is purely elastic, then:

$$\delta = 0, \sin\delta = 0, \text{ and } \Delta U = 0 \quad (6)$$

If the response to a stress is purely viscous, then γ_{max} consists entirely of permanent strain, and:

$$\delta = 90, \sin\delta = 1, \text{ and } \Delta U \propto \gamma_{max} \quad (7)$$

Two changes to equation (5) were made when developing the binder specification. First, the absolute value symbols for G* were dropped. G* is the complex shear modulus that is a vector containing an imaginary element, while $|G^*|$ is the dynamic shear modulus that is a scalar containing no imaginary element. Normally, when the absolute value symbols are dropped, $|G^*|$ is described simply as G, which is called the dynamic shear modulus. In Superpave only the absolute value symbols were dropped for simplification purposes. Technically, the term should be described as $|G^*|$.

Second, because most asphalt paving technologists have some understanding of the term "modulus," the parameter $\sin\delta/G^*$ was inverted to $G^*/\sin\delta$ for

convenience. Based on dissipated energy, $G^*/\sin\delta$ is inversely proportional to the energy dissipated by the viscous flow component of the strain; therefore, as $G^*/\sin\delta$ increases, rutting susceptibility should decrease.

b. $G^*/\sin\delta$'s of the Binders Corresponding to the ALF Pavement Tests

Samples of the five binders were aged using the RTFO and tested by the DSR to determine $G^*/\sin\delta$ as a function of temperature and angular frequency.[14] All tests were performed in the linear viscoelastic range. For DSR tests at 40 °C and higher, a 1-mm gap and 25-mm diameter plates were used. For tests below 40 °C, a 2-mm gap and 8-mm diameter plates were used. As expected, $G^*/\sin\delta$ decreased with an increase in temperature and with a decrease in angular frequency.

The $G^*/\sin\delta$'s of the five binders at the pavement test temperature of 58 °C and an angular frequency of 2.25 rad/s were obtained. These $G^*/\sin\delta$'s were compared with the ALF pavement test results. A DSR angular frequency of 2.25 rad/s was chosen based upon a vehicle speed of 80 km/h being equivalent to the standard DSR angular frequency of 10.0 rad/s. Therefore, the speed of the ALF, which was 18 km/h, was divided by 8.0 km/h per rad/s to obtain a DSR angular frequency of 2.25 rad/s. This frequency, which accounts for the relatively slow speed of the ALF, is called the "ALF angular frequency" in this report. The $G^*/\sin\delta$'s of the binders at the standard angular frequency of 10.0 rad/s and at 2.25 rad/s are given in table 12 and figures 4 and 5. (Authors' note: Superpave currently equates a vehicle speed of 100 km/h to 10.0 rad/s, whereas, 80 km/h was equated to 10.0 rad/s by Superpave when this study started. This change was made without the addition of new data and is inconsequential. The relationship between vehicle speed and DSR angular frequency is inherent in the test method.)

A frequency of 10.0 Hz, which is equivalent to a total loading time of 0.1 s/cycle, is used in most repeated load mixture tests for fatigue cracking and rutting. The peak load occurs at 0.05 s. This loading time has been in use for more than 30 years. It was based on a vehicle speed of 80 ±10 km/h (22 ±3 m/s) and an average pavement deflection basin length of 2.2 m:

$$\text{time} = \text{distance/speed} = 2.2\ \text{m}/22\ \text{m/s} = 0.1\ \text{s}$$

Because the loading time of 0.1 s is based on an average deflection basin due to pavement bending, it is reasonable to assume this loading time can be used in repeated load tests for fatigue cracking. (The applicability of using 2.2 m vs. some other length is a separate issue.) Whether the entire deflection basin should be used to establish the loading time for rutting tests can be questioned, but 0.1 s is the loading time most commonly used for repeated load compression and shear tests for rutting. Based on physics and a loading time of 0.1 s, the angular frequency for the DSR should be:

$$\omega = 2\pi f = 2\pi/t = (6.28\ \text{rad/cycle})/(0.1\ \text{s/cycle}) = 62.8\ \text{rad/s}$$

where: ω = angular frequency, rad/s
2π = conversion, rad/cycle
f = frequency = 1/t, Hz, or cycles/s
t = time period of one cycle, s/cycle

Superpave should use a standard frequency of 62.8 rad/s. The use of 10.0 rad/s in lieu of 62.8 rad/s means that Superpave equates 10.0 rad/s to 10.0 Hz to 80 km/h (or 100 km/h). No justification for this discrepancy is known. It was decided to use an angular frequency of 2.25 rad/s, which was based on a vehicle speed of 80 km/h being equivalent to the standard DSR angular frequency of 10.0 rad/s.

When comparing the $G^*/\sin\delta$'s given in table 12 with each other, it should be kept in mind, that as the test temperature decreases, at some temperature the rheological properties of the binders will change such that the parameter $G^*/\sin\delta$ is no longer a valid measure of rutting susceptibility. This temperature is unknown and should vary from binder to binder. Because no rest period is used in the DSR test, the time dependent recoverable strain (delayed elastic strain) that would be recovered if a rest period were to be included, is measured as permanent strain by the DSR. The amount of time dependent recoverable strain should decrease with an increase in temperature, and should be negligible for unmodified binders at the test temperatures used to grade these binders. This warning also applies to figures 4 and 5. The data in table 2 of chapter 1 should be used to compare the moderate and low temperature properties of the binders.

2. Background for the ALF Pavement Tests

The ALF consists of a structural frame, 29 m in length, containing a moving wheel assembly. The wheel assembly models one-half of a single rear truck axle and can apply loads ranging from 44.5 to 100.1 kN. Approximately 8,600 wheel passes can be applied per day if no distress surveys are needed; 50,000 wheel passes can be applied per week, which includes time for maintenance. To simulate highway traffic, the ALF loads the pavement in one direction. The loads can also be distributed from side to side to simulate traffic wander. The ALF is computer controlled, permitting a 24-h operation. The ALF is shown in figures 6 and 7. Additional information on the ALF is given in appendix A.

The ALF in the rutting study was operated according to the following characteristics:

- Super single tire with a tire pressure of 690 kPa.
- Load of 43 kN.
- No lateral wheel wander.
- Speed of 18.5 km/h.
- Total wheelpath length of 13.7 m (the distress surveys are performed on a 10-m section).
- An infrared heating system and thermocouples in the pavements provided the required pavement temperature at the required pavement depth.

Table 12. G*/sinδ after RTFO vs. temperature and angular frequency.

Temp. (°C)	AC-5	AC-10	AC-20	Novophalt	Styrelf
G*/sinδ at 10.0 rad/s, Standard Angular Frequency for the DSR, Pa:					
10	5 172 000	11 990 000	17 880 000	26 390 000	22 550 000
20	862 000	2 001 000	3 074 000	5 603 000	5 106 000
30	173 100	386 600	666 300	1 154 000	1 053 000
40	38 640	82 800	159 900	263 600	270 900
50	7 528	15 880	30 660	60 150	75 960
58	2 600	5 285	10 010	21 090	35 170
60	2 096	4 202	7 897	16 580	28 504
70	653	1 238	2 226	4 965	11 380
G*/sinδ at 2.25 rad/s, Angular Frequency for the ALF, Pa:					
10	2 240 000	5 364 000	8 335 000	12 560 000	11 074 118
20	351 800	833 500	1 383 000	2 279 000	2 294 000
30	62 220	143 900	267 700	425 400	466 900
40	11 910	26 350	54 470	92 470	117 700
50	2 057	4 446	9 002	19 140	31 790
58	664	1 384	2 702	6 826	13 710
60	526	1 084	2 100	4 914	11 570
70	155	299	549	1 306	4 435

Table 13. High-temperature continuous PG at the standard DSR angular frequency of 10 rad/s and the ALF angular frequency of 2.25 rad/s.

Conventional Designation:	AC-5	AC-10	AC-20	Novo-phalt	Styrelf
At G*/sinδ = 2.20 kPa, 10.0 rad/s, °C	59	65	70	77	88
At G*/sinδ = 2.20 kPa, 2.25 rad/s, °C	50	56	59	66	77
Temperature Difference, °C	9	9	11	11	11
Average Temperature Difference = 10 °C					

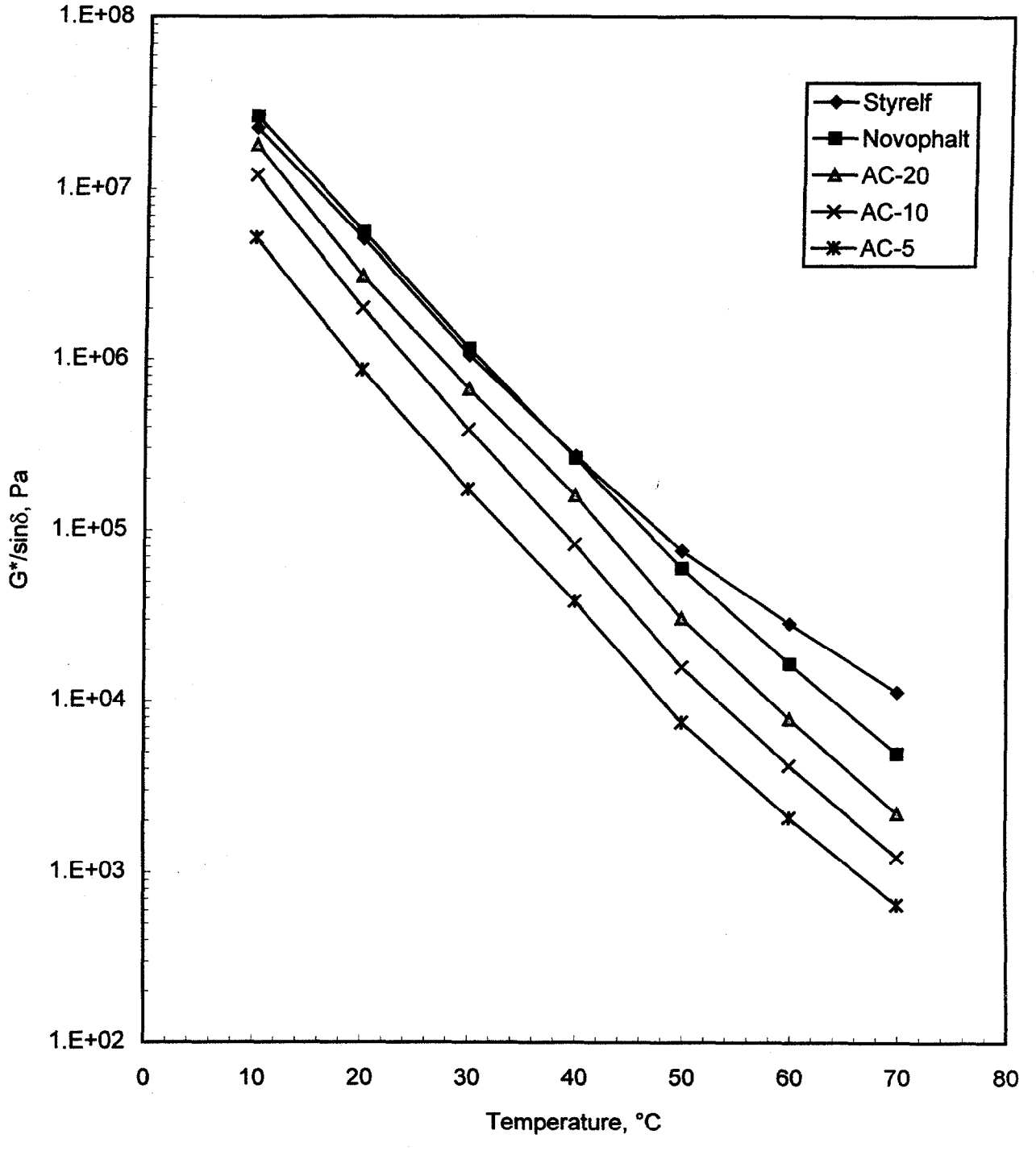

Figure 4. G*/sinδ vs. temperature at a DSR frequency of 10.0 rad/s.

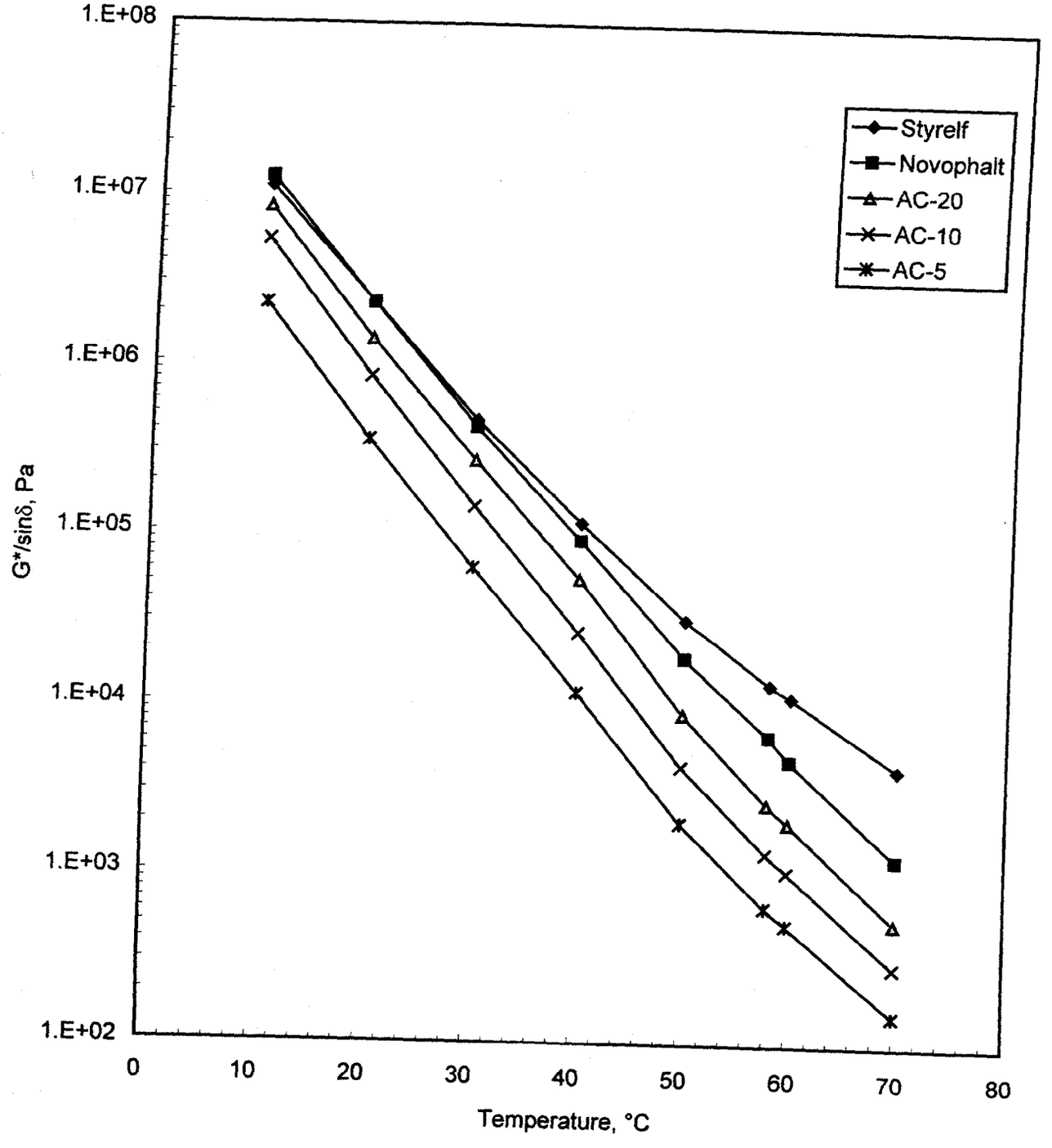

Figure 5. G*/sinδ vs. temperature at a DSR frequency of 2.25 rad/s.

Figure 6. The FHWA Accelerated Loading Facility and typical ruts in the pavements.

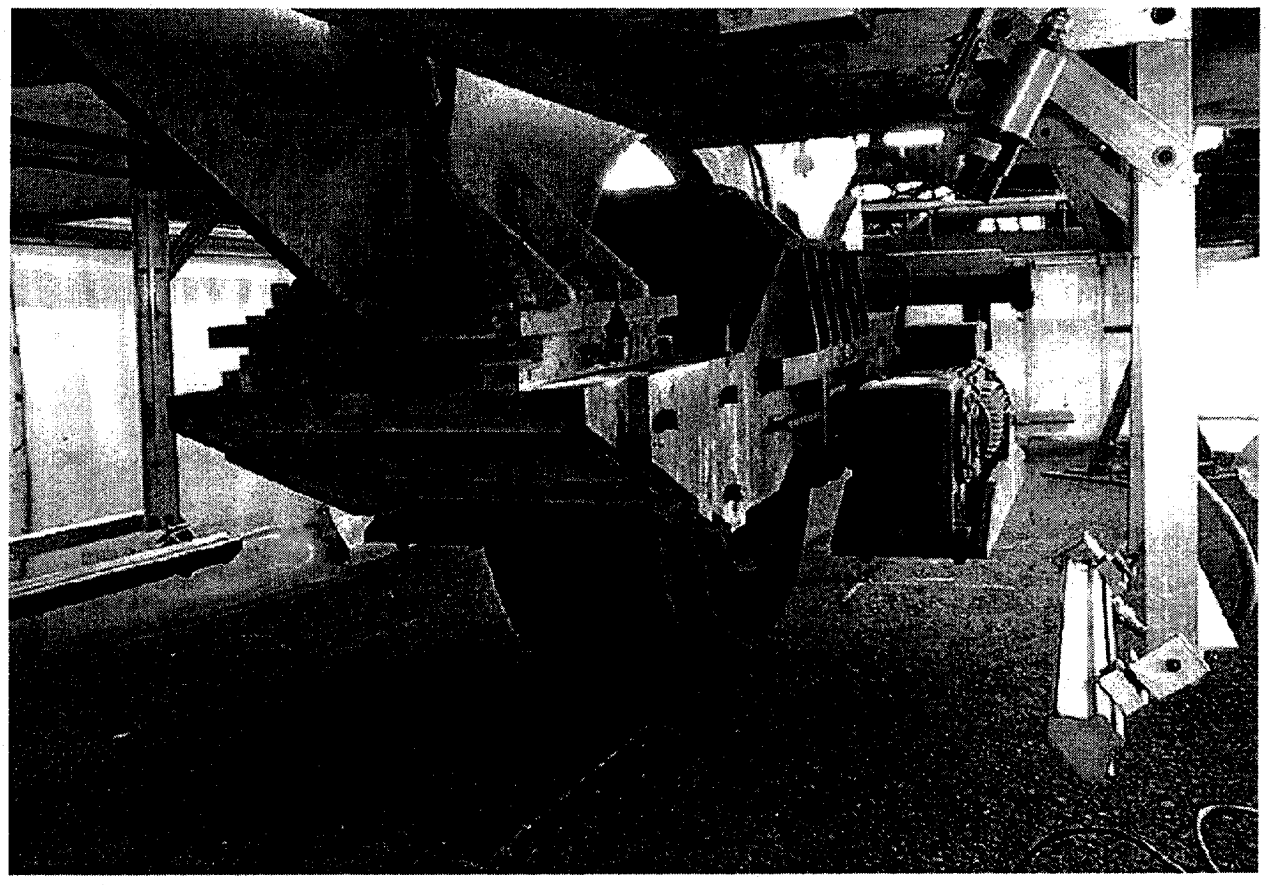

Figure 7. Close-up of the ALF super single tire and heat lamps on the right and left sides of the tire.

A super single tire and no wander were chosen in lieu of a dual wheel tire and wander so that the data collected in this study could be used to develop or refine performance prediction models in future studies. This type of loading is the easiest to model. The following data were collected:

- Temperature of the asphalt pavement layer versus depth.
- Transverse and longitudinal surface profiles.
- Crack mapping.
- Deformations in underlying layers.
- Core properties in and out of the wheelpath.
- Profiles after trenching.

Pavement temperature was controlled during trafficking using infrared lamps attached to the bottom of the ALF frame. Temperatures at pavement depths of 0, 20, 102, and 197 mm were recorded by thermocouples at two locations outside, but close to, the wheelpath. A target temperature of 70 °C at a depth of 20 mm was initially chosen so that the pavement tests would be performed at a temperature near the middle of the high-temperature PG's of the five binders. However, the Superpave binder specification is based on traffic speeds of 80 to 100 km/h while the ALF travels at 18 km/h. Therefore, the slow speed of the ALF would make the pavement tests too severe at 70 °C. Table 13 provides the temperatures of the five binders at a $G^*/\sin\delta$ of 2.20 kPa and frequencies of 10.0 and 2.25 rad/s. According to the temperatures in table 13, a test performed at 2.25 rad/s and a selected temperature is equivalent to a test performed at 10 rad/s and a 10 °C higher temperature. Assuming this relationship is applicable to the ALF, an ALF pavement test at 58 °C and 18 km/h is equivalent to an ALF pavement test at 68 °C if the speed could be increased to 80 to 100 km/h. Because of this, the target temperature was reduced approximately two grades to 58 °C. This is equivalent to the shift in high-temperature PG for "standing" traffic loadings, defined as less than 20 km/h in the 1998 AASHTO provisional standard MP2.[3] The temperature at a depth of 20 mm was controlled in this study because Superpave recommended that the temperature at this depth be used to represent the temperature of a pavement.[15] The locations for the thermocouples are shown in figure 8.

All seven mixtures were tested at 58 °C in 1994. Tests at 58 °C were repeated in 1995 on the pavements with the AC-5 and AC-20 (PG 59 and 70) surface mixtures and the AC-5 (PG 59) base mixture to determine the repeatability of the ALF data. These three pavements were chosen because after the seven pavements were tested, the ALF rutting performances of the poorest performing pavements, which included these three pavements, were close to each other. The ALF rutting performances of the best performing pavements were distinctly different.

A minimum of seven distress surveys was performed on each pavement during trafficking using Long-Term Pavement Performance distress survey methods.[16] The surveys included transverse profiles, longitudinal profiles, and the number and severity of cracks. A rut depth of 20 mm in the asphalt pavement layer was defined as the failure point for the rutting studies. This rut

depth is equivalent to 10 percent strain, and it was measured based on the initial pavement surface elevation. The measurement did not include any upward heaving outside the wheelpath.

After pavement failure, three 152.4-mm diameter cores were taken from the wheelpath and eight 152.4-mm cores were taken outside the wheelpath to determine air voids and densification, and to verify asphalt pavement layer thickness, rut depth, binder content, aggregate gradation, and maximum specific gravity. The thicknesses of the lifts in and out of the wheelpath were measured to estimate how much permanent deformation occurred in each lift. The surface mixtures were placed in four lifts while the base mixtures were placed in two lifts. The locations for the cores are shown in figure 8.

The rut depth in the asphalt pavement layer alone was measured during each distress survey using a survey rod and level. After the crushed aggregate base layer was compacted during construction, aluminum plates were attached to its surface using nails at three locations in the wheelpath. Before each pavement site was tested by the ALF, holes were drilled through the asphalt pavement layer to each plate. A short reference rod was then screwed into each plate. During each distress survey, a metal rod connected to the bottom of a survey rod was put into each hole and placed on top of the reference rod. A survey level was then used to determine the distance the plate had moved downward. This provided the amount of rutting in the underlying layers, which was subtracted from the total rut depth to determine the amount of rutting in the asphalt pavement layer alone. The amount of rutting in the underlying layers was desired to be negligible. The locations for the reference rods and plates are shown in figure 8. A sketch of the device is shown in figure 9.

3. ALF Pavement Tests Results at 58 °C

The only pavement test temperature that was used for all seven mixtures was 58 °C. The large differences in performance from mixture to mixture coupled with large changes in performance with a change in temperature prohibited testing all seven mixtures at another, single temperature.

a. Temperature and Material Properties

The average pavement temperatures during trafficking for each lane and at each depth are given in table 14. The average temperatures based on the data from all lanes at depths of 0, 20, 102, and 197 mm were 60, 58, 56, and 51 °C, respectively. Rankings for $G^*/\sin\delta$ at these temperatures and the ALF angular frequency of 2.25 rad/s are given in table 15. These rankings were determined using Fisher's Least Significant Difference (LSD) statistical procedure. Fisher's LSD determines which averages are not significantly different from other averages. Averages that are not significantly different are grouped together. The groups are then ranked from highest to lowest and coded with a letter. Binders that fall into more than one group will have more than one letter assigned to it. Fisher's LSD is performed in conjunction

with an analysis of variance at a 95-percent confidence level. The letter "A" indicates the highest $G^*/\sin\delta$. The $G^*/\sin\delta$'s of the five binders were significantly different at all four temperatures.

Even though the target temperature of 58 °C was met based on the overall average temperature, table 14 shows that the range in average temperature at a depth of 20 mm from lane to lane was 55 to 60 °C. How these differences in temperature affected the rut depths was not quantitatively known, and thus could not be taken into account. The temperatures from all lanes at a depth of 20 mm provided 95-percent confidence limits of 58 ±4 °C based on two times the sample standard deviation, $\pm 2\sigma_{(n-1)}$, where "n" is the number of samples.

The average air voids are given in table 14. The as-constructed air voids of the pavements, based on cores taken from out of the wheelpath, differed by as much as 6 percent from lane to lane. Construction specifications were developed to provide low lane-to-lane variability in material composition. This included air voids, aggregate gradation, and binder content. The intent of this specification was not achieved in terms of air voids.

Table 14 includes the decrease in air voids, or densification, due to trafficking. By comparing the densification in the top half of each asphalt pavement to that of the bottom half, it was found that they were virtually the same for five out of seven mixtures. More densification occurred in the top half (3.4 percent) of the Novophalt surface mixture than in its bottom half (1.8 percent). Unexpectedly, less densification occurred in the top half (2.9 percent) of the AC-10 (PG 65) surface mixture than in its bottom half (5.1 percent). The average densification based on the data from all lanes was 3.8 percent in both the top and bottom halves. Regression analyses using the data from all mixtures or from the surface mixtures only showed that $G^*/\sin\delta$ and amount of densification did not correlate ($r^2 = 0$). Aggregate gradation also appeared to have little to no effect on densification.

The average decrease in air voids due to trafficking ranged from 2.4 percent for lane 12 to 5.2 percent for lane 10. Multiplying these values by the asphalt pavement layer thickness of 200 mm gives a range in rut depth from 4.8 to 10.4 mm. Dividing these values by the average rut depth of 24 mm for all lanes at termination suggests that 20 to 44 percent of the 24-mm rut depth was densification. As the percent rut depth from densification increases, the percent rut depth from viscous flow decreases, and vice versa. However, the results from these calculations could be in error. The air voids in the wheelpaths were only determined after the pavements had failed, and the pavement tests were not terminated solely on some scientific basis, such as some fixed amount of rutting in the asphalt pavement layer. In fact, some of the final rut depths differed by more than 10 mm. Because of this, the differences in densification from lane to lane was a confounding factor that could not be adequately taken into account.

The aggregate gradations, binders contents, and maximum specific gravities of samples acquired during construction and from pavement cores taken after pavement failure are given in appendix B.

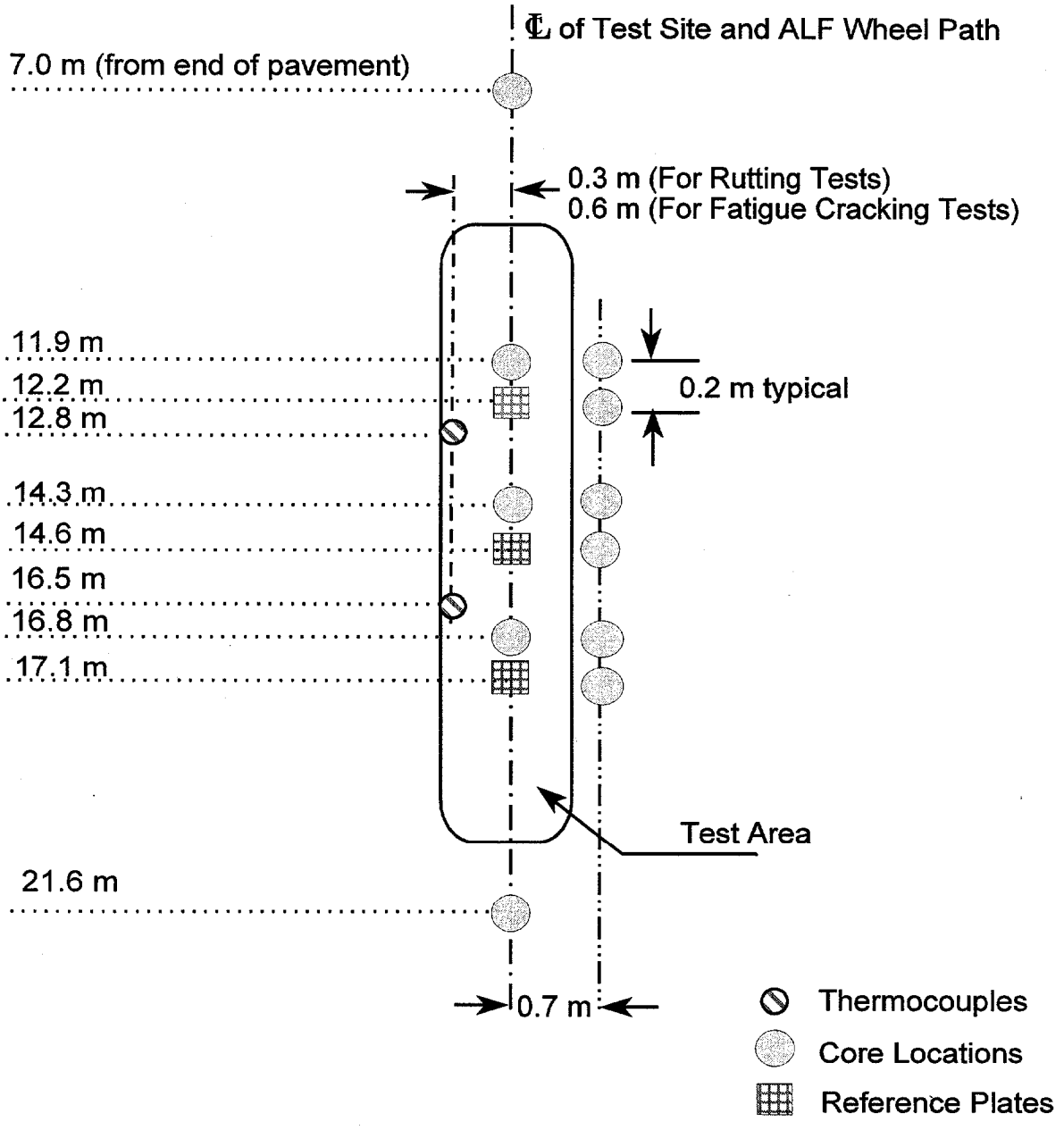

Figure 8. Thermocouple, core, and reference plate locations for each site.

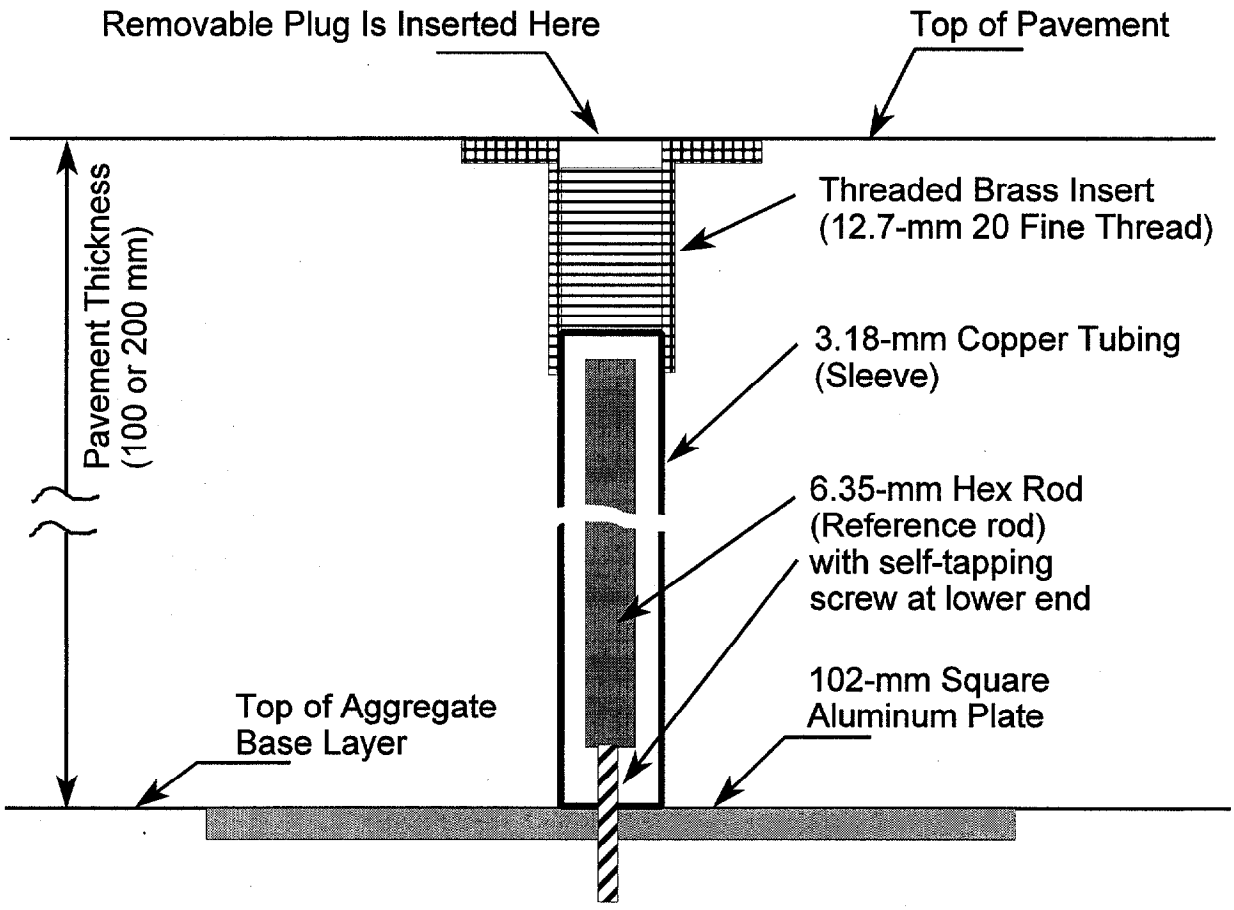

Figure 9. Drawing of the reference rod used to measure the amount of rutting in the layers below the asphalt pavement layer.

Table 14. Pavement temperatures and air voids.

	Surface Mixture					Base Mixture	
Pre-Superpave:	AC-5	AC-10	AC-20	Novophalt	Styrelf	AC-5	AC-20
Superpave PG:	59	65	70	77	88	59	70
Lane Number:	9	5	10	8	7	11	12
Pavement Depth	**Pavement Temperature, °C**						
0 mm	62	62	60	56	61	60	59
20 mm	58	60	58	55	59	58	57
102 mm	55	55	55	54	59	56	56
197 mm	51	49	51	48	56	51	51
Difference from 0 mm to 197 mm:	11	13	9	8	5	9	8
	Air Voids, Top 100 mm of Pavement, Percent						
Out of Wheelpath	7.8	8.5	9.1	11.9	11.9	6.7	7.4
In Wheelpath	3.4	5.6	3.7	8.5	7.6	3.1	5.0
Decrease	4.4	2.9	5.4	3.4	4.3	3.6	2.4
	Air Voids, Bottom 100 mm of Pavement, Percent						
Out of Wheelpath	7.0	8.4	8.3	10.8	12.8	6.0	7.4
In Wheelpath	2.8	3.3	3.4	9.0	8.2	2.2	5.1
Decrease	4.2	5.1	4.9	1.8	4.6	3.8	2.3
Average Decrease for Entire Layer	4.3	4.0	5.2	2.6	4.4	3.7	2.4

G*/sinδ for the Novophalt and Styrelf Surface Mixtures at 2.25 rad/s, Pa

Pavement Depth, mm	Novophalt Temp, °C	Novophalt G*/sinδ	Styrelf Temp, °C	Styrelf G*/sinδ	Comparison of G*/sinδ (by *t*-test)
0	56	8 300	61	10 550	Novophalt < Styrelf
20	55	9 680	59	12 590	Novophalt < Styrelf
102	54	11 140	59	12 590	Novophalt ≈ Styrelf
197	48	26 510	56	18 070	Novophalt > Styrelf

Table 15. G*/sinδ after RTFO corresponding to the ALF pavements tests.[1]

Pre-Superpave Designation:	AC-5	AC-10	AC-20	Novo-phalt	Styrelf
Superpave PG:	59	65	70	77	88
G*/sinδ at 60 °C, and 2.25 rad/s (18 km/h), Pa	526 E	1 084 D	2 100 C	4 914 B	11 570 A
G*/sinδ at 58 °C, and 2.25 rad/s (18 km/h), Pa	664 E	1 384 D	2 702 C	6 826 B	13 710 A
G*/sinδ at 56 °C, and 2.25 rad/s (18 km/h), Pa	872 E	1 833 D	3 632 C	8 296 B	17 620 A
G*/sinδ at 51°C, and 2.25 rad/s (18 km/h), Pa	1 813 E	3 892 D	7 918 C	17 560 B	29 030 A

[1]The letters "A" through "E" are the statistical ranking, with "A" denoting the highest G*/sinδ.

b. Rut Depths

(1) Rut Depth vs. ALF Wheel Pass Relationships Using the Raw Data and a Rut Depth Model

The rut depths in the asphalt pavement layer and the total rut depths were fitted according to the following rut depth model using the Gauss-Newton statistical method:

$$RD = aN^b$$

where:

RD = rutting depth in asphalt pavement layer or all layers, mm;
N = ALF wheel passes;
a = intercept, and
b = slope.

The rut depths up to 10,000 ALF wheel passes are shown in figures 10 through 13. As stated previously, these rut depths are based on the original elevation of the pavement surface before testing. Figure 10 shows the measured rut depths in the asphalt pavement layer while figure 11 shows the rut depths in the asphalt pavement layer using the above rut depth model. Figures 12 and 13 show the same relationships using the total rut depth, which is the rut depth in all pavement layers. The rut depth model was used to provide a smooth relationship between rut depth and wheel passes.

Table 16 shows the wheel passes at rut depths of 15 and 20 mm based on the raw data and the rut depth model. The large differences in wheel passes provided by these two methods for the pavement with Styrelf was the result of having to obtain the wheel passes where the slope was low. When the slope in terms of rut depth per wheel pass is low, the error in wheel passes at a given rut depth is high, and the ability of the method to accurately define the relationship between rut depth and wheel passes becomes extremely important. Extrapolations include, and can magnify, the error. Subsequent analyses performed in this study are based on the relationships from the rut depth model.

Table 16 also shows that fewer than 3,000 ALF wheel passes were required to obtain a rut depth of 20 mm for the three surface mixtures with the unmodified binders. This shows that the change in target pavement test temperature from 70 to 58 °C, which was done to account for the slow speed of the ALF, was necessary. Tests at 70 °C would be too severe for these three pavements.

(2) Comparison of the Rut Depth in the Asphalt Pavement Layer to the Total Rut Depth

The ALF wheel passes at rut depths of 10, 15, and 20 mm are given in table 17. As expected, the wheel passes based on the rut depth in the asphalt pavement layer alone were higher than those based on the total rut depth. These differences were attributed to rutting in the crushed aggregate base. The differences were very high for the two mixtures with modified binders. For example, 23,200 wheel passes were needed to obtain a total rut depth

of 20 mm in lane 7 with Styrelf, whereas approximately 220,000 wheel passes would be needed to obtain this same rut depth in the asphalt pavement layer alone. Based on a maximum allowable total rut depth of 20 mm, the data indicate that lanes 7 and 8 with the modified binders failed before a significant amount of rutting occurred in the asphalt pavement layer. These pavements also exhibited no upward heaving outside the wheelpath. The pavements with the unmodified binders did heave. This shows that even though the two modified binders drastically increase pavement life on the basis of the rut depths in the asphalt pavement layer, a significantly longer pavement life on the basis of total rut depth would have been obtained if the asphalt pavement layer was thicker than the 200-mm layer that was placed. A more stable crushed aggregate base layer should also increase pavement life based on total rut depth. Table 17 includes the percent rut depth in the asphalt pavement layer. The pavements with the modified binders had the lowest percentages.

(3) Statistical Rankings for the Pavements

The rut depths in the asphalt pavement layer were used to rank the mixtures. To statistically rank the mixtures according to rutting susceptibility, the average variability in rut depth provided by lanes 9, 10, and 11 had to be applied to the other four lanes. Only these three lanes were tested in both 1994 and 1995. The data in tables 14 and 17 for these lanes are the average data. The replicate data are given in table 18.

The replicate data from lanes 9, 10, and 11 provided two relationships for each lane: the average rut depth (RD_{avg}) vs. wheel pass and two standard deviations of the rut depth ($2\sigma_{(n-1)}$) vs. wheel pass. The latter relationship provided 95-percent confidence bands for the rut depths in the form of $RD_{avg} \pm 2\sigma_{(n-1)}$. A relationship between $2\sigma_{(n-1)}$ and RD_{avg} using the data from all three replicated pavement tests was computed. This relationship is shown in figure 14. The variability in rut depth, expressed as $\pm 2\sigma_{(n-1)}$, increased with an increase in RD_{avg} and was nearly linear:

$$2\sigma_{(n-1)} = 0.221416(RD)^{1.04465} \qquad r^2 = 0.72$$

where:

$2\sigma_{(n-1)}$ = two times the standard deviation of the rut depths, where the sample variance was used, and
Rd_{avg} = average rut depth in the asphalt pavement layer.

Each ALF pavement test provided a relationship between rut depth and ALF wheel passes. To rank the seven mixtures, 95-percent confidence bands were determined for each mixture by substituting the rut depths for RD_{avg} in the above equation and calculating $2\sigma_{(n-1)}$. The confidence bands were computed using the rut depth $\pm 2\sigma_{(n-1)}$. For each of the three lanes that were tested twice, the rut depths at each wheel pass were first averaged. The confidence bands were then applied to these averages. When the confidence bands of the mixtures overlapped at the higher numbers of wheel passes, it was concluded that the rut depths were not significantly different. The rankings based on the $\pm 2\sigma_{(n-1)}$ confidence bands are given in table 19. The rut depth data from

the beginning to the end of each test are given in appendix C. For the five surface mixtures, table 19 shows that only the AC-10 and AC-20 (PG 65 and 70) mixtures were not significantly different. However, this ranking cannot be considered exact and undisputable because of the poor r^2 of 0.72 for the relationship shown in figure 14. Rankings based on $\pm 1\sigma_{(n-1)}$ are included in table 19 as supplementary information.

A second method for statistically ranking the mixtures, based on an average coefficient of variation, was also used. This method consisted of calculating an average coefficient of variation in terms of wheel passes at a rut depth of 20 mm using the three pairs of replicate rut depths. This coefficient of variation was found to be 0.22. Replicate ALF wheel passes at a rut depth of 20 mm for all seven mixtures were then calculated using this coefficient.

As shown by table 20, the sample standard deviation was calculated by multiplying the average wheel pass times 0.22. The sample standard deviation and the average wheel pass were then used to calculate two replicate wheel passes. A normal distribution was assumed. The mixtures were then ranked using analyses of variance and Fisher's LSD. Log wheel passes were ranked because the sample standard deviation increased with an increase in wheel passes. Table 20 shows that the ranking for the five surface mixtures at a rut depth of 20 mm was identical to the ranking provided by the $\pm 1\sigma_{(n-1)}$ and $\pm 2\sigma_{(n-1)}$ confidence bands in table 19. Only the AC-10 and AC-20 (PG 65 and 70) mixtures were not significantly different. Tables 19 and 20 show that the rankings provided by the two methods using all seven mixtures were different. Rankings at rut depths of 10 and 15 mm are included in table 20. A slightly different ranking for the five surface mixtures was obtained at a rut depth of 10 mm.

Like the first method for ranking the mixtures, the second ranking method cannot be considered exact and undisputable. The coefficients of variation provided by the three replicated pavement tests at a 20-mm rut depth were 0.31, 0.00, and 0.35. This provided the average coefficient of 0.22. If a coefficient of variation of 0.33 were to be used instead of 0.22, the wheel passes for the mixtures with the AC-5 and AC-10 (PG 59 and 65) binders would not be significantly different.

(4) Comparisons of the Rut Depths at Various Wheel Passes

Comparing the rut depths at various ALF wheel passes was found to be problematic because the pavements failed at widely different wheel passes. The wheel passes at a rut depth of 20 mm in the asphalt pavement layer ranged from 670 to more than 200,000. Either excessive extrapolations leading to very high rut depths would have to be applied to the data from pavements that failed quickly, or the pavements would have to be compared at very low numbers of wheel passes. At low wheel passes, the poorest performing pavements control how a set of mixtures will rank, and the rut depths for the best performing mixtures tend to be the same regardless of test temperature. Comparisons based on the rut depths at a specific number of wheel passes were

used in this study when appropriate. Comparisons at 2,000 wheel passes for pavement tests at 58 and 70 °C have been previously reported.[17,18]

c. Pavement Cracks

Cracks were only observed in the lane with the Novophalt (PG 76-22) mixture. Thin longitudinal cracks were observed on the pavement surface on both sides of the wheelpath at the point where the pavement was bending the greatest. All cracks initiated at the surface of the pavement.

4. Validation of G*/sinδ Based on the ALF Pavement Data From the Five Surface Mixtures

The two rankings in table 21 show a reversed order for Novophalt and Styrelf. The G*/sinδ of Styrelf was higher than the G*/sinδ of Novophalt, but the Novophalt mixture was least susceptible to rutting. Table 14 shows that the temperatures of the pavement with Novophalt were lower than those for Styrelf. The corresponding G*/sinδ's are included at the bottom of table 14. Statistical analyses of the G*/sinδ's showed that, at depths of 0 and 20 mm, the G*/sinδ's of the Novophalt binder were still significantly lower than those for Styrelf. However, the G*/sinδ's were not significantly different at 102 mm, while the G*/sinδ of the Novophalt binder was significantly higher than for Styrelf at 197 mm. This confounded the experiment but did not clearly explain the reversal.

The data are shown graphically in figure 15. The r^2 between log ALF wheel passes and G*/sinδ for the five surface mixtures was 0.34. Therefore, the degree of correlation was very poor. The r^2 for the seven mixtures was 0.32.

5. Validation of G*/Sinδ Based on the Data From the AC-5 and AC-20 (PG 59 and 70) Surface and Base Mixtures

a. Effect of Nominal Maximum Aggregate Size on Rutting Susceptibility

The wheel passes needed to produce a 20-mm rut depth in the AC-5 and AC-20 (PG 59 and 70) surface and base mixtures were examined. These data are included in table 17. The AC-5 (PG 59) base mixture required 11,990 wheel passes compared with 670 wheel passes for the AC-5 (PG 59) surface mixture. The base mixture increased the required wheel passes by 1,700 percent. The AC-20 (PG 70) base mixture required 57,520 wheel passes compared with 2,730 wheel passes for the AC-20 (PG 70) surface mixture. This base mixture increased the required wheel passes by 2,000 percent. Decreases in rutting susceptibility due to the increase in nominal maximum aggregate size also occurred at rut depths of 10 and 15 mm. Increased nominal maximum aggregate size and the associated 0.85-percent decrease in optimum binder content significantly decreased rutting susceptibility for both binder grades.

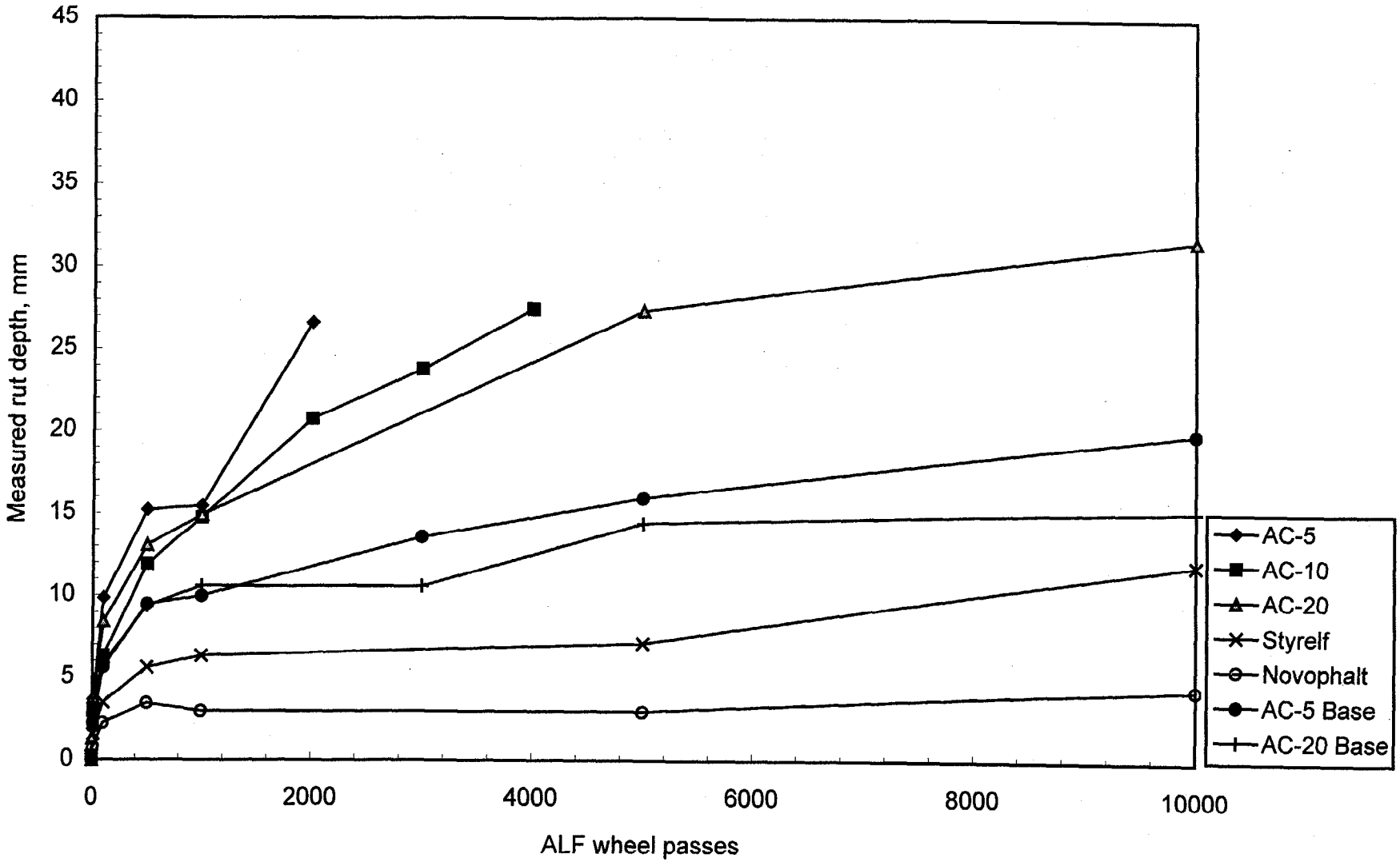

Figure 10. Measured rut depth in the asphalt pavement layer vs. ALF wheel passes.

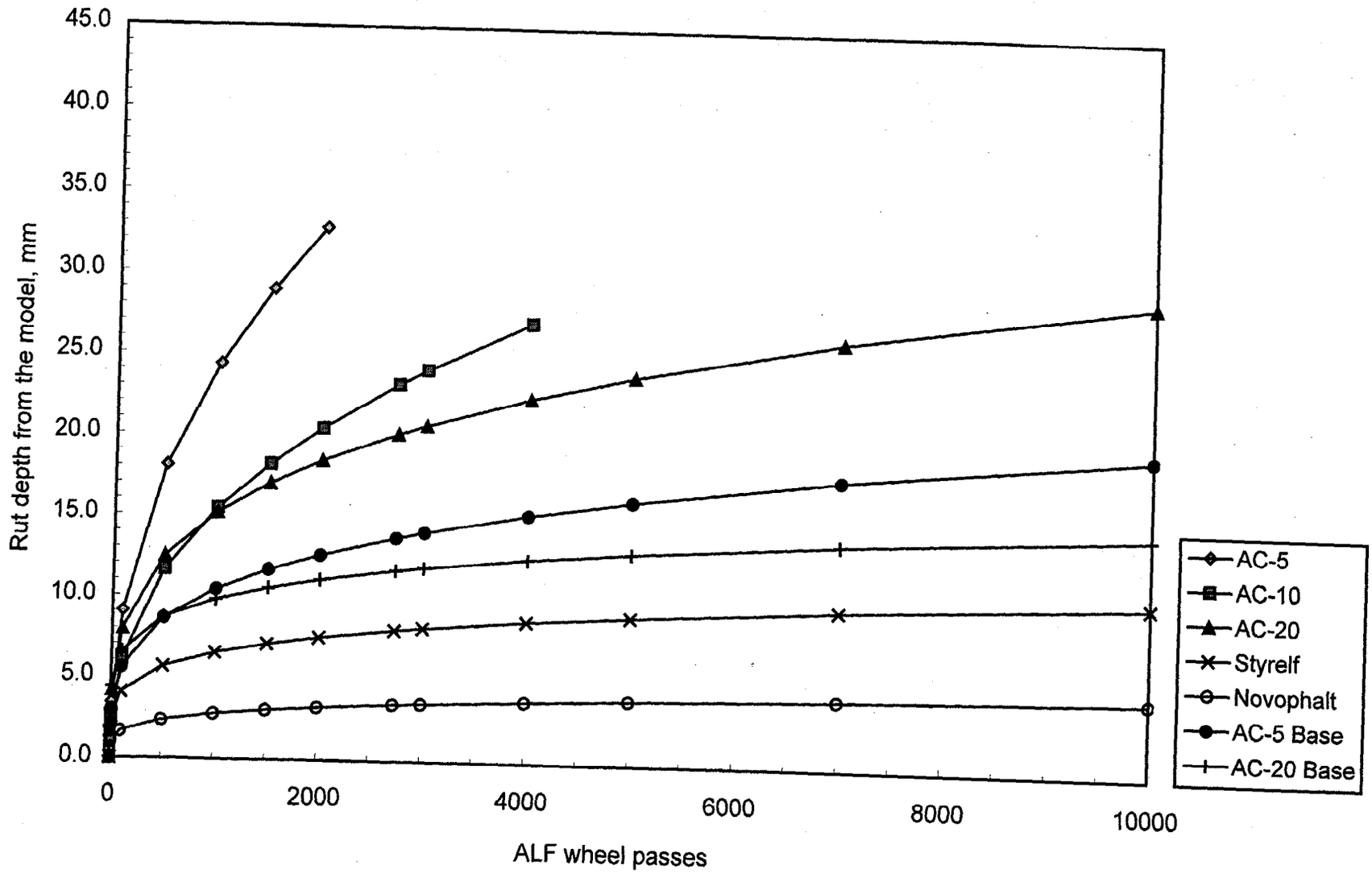

Figure 11. Rut depth in the asphalt pavement layer from the model vs. ALF wheel passes.

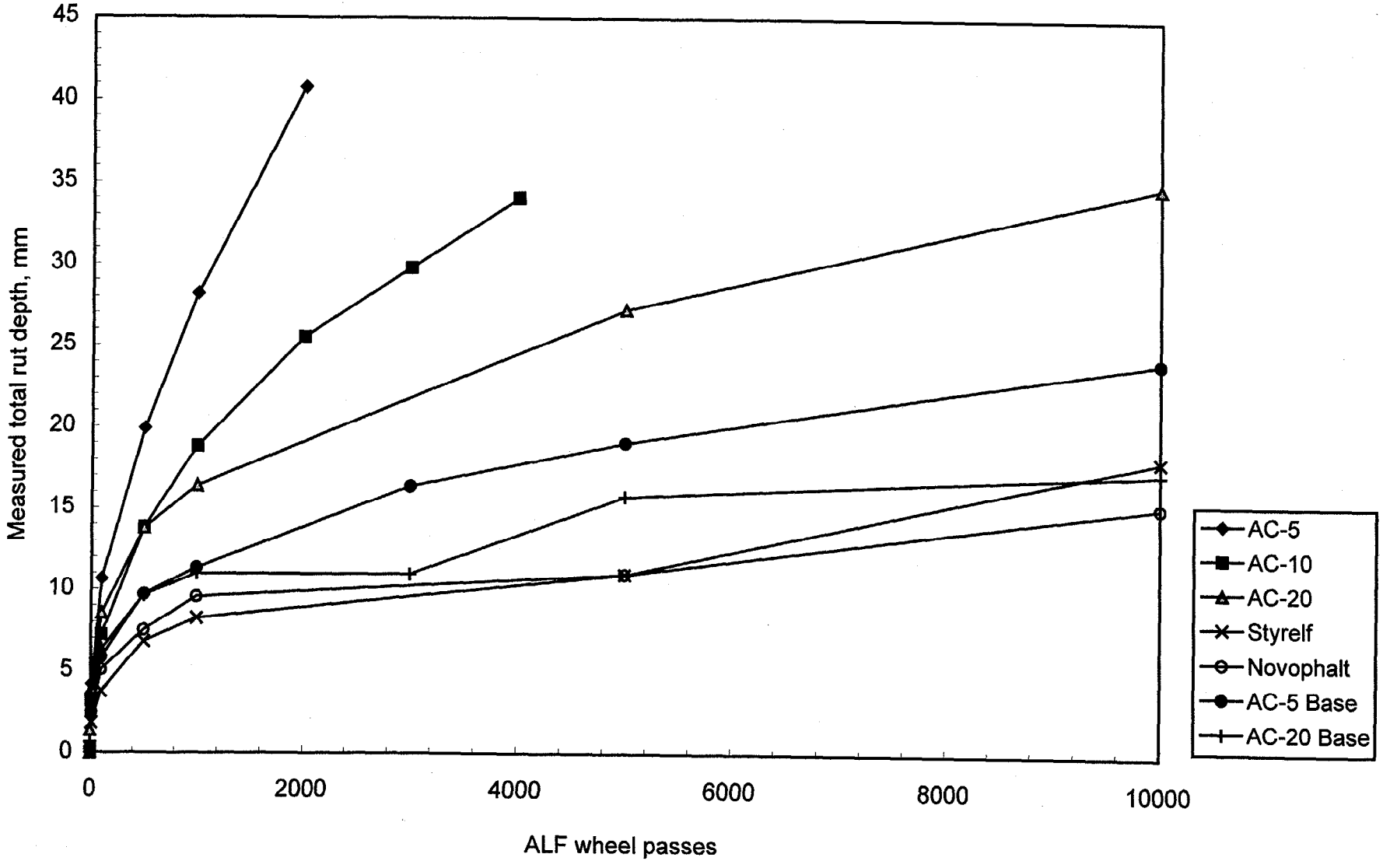

Figure 12. Measured total rut depth vs. ALF wheel passes.

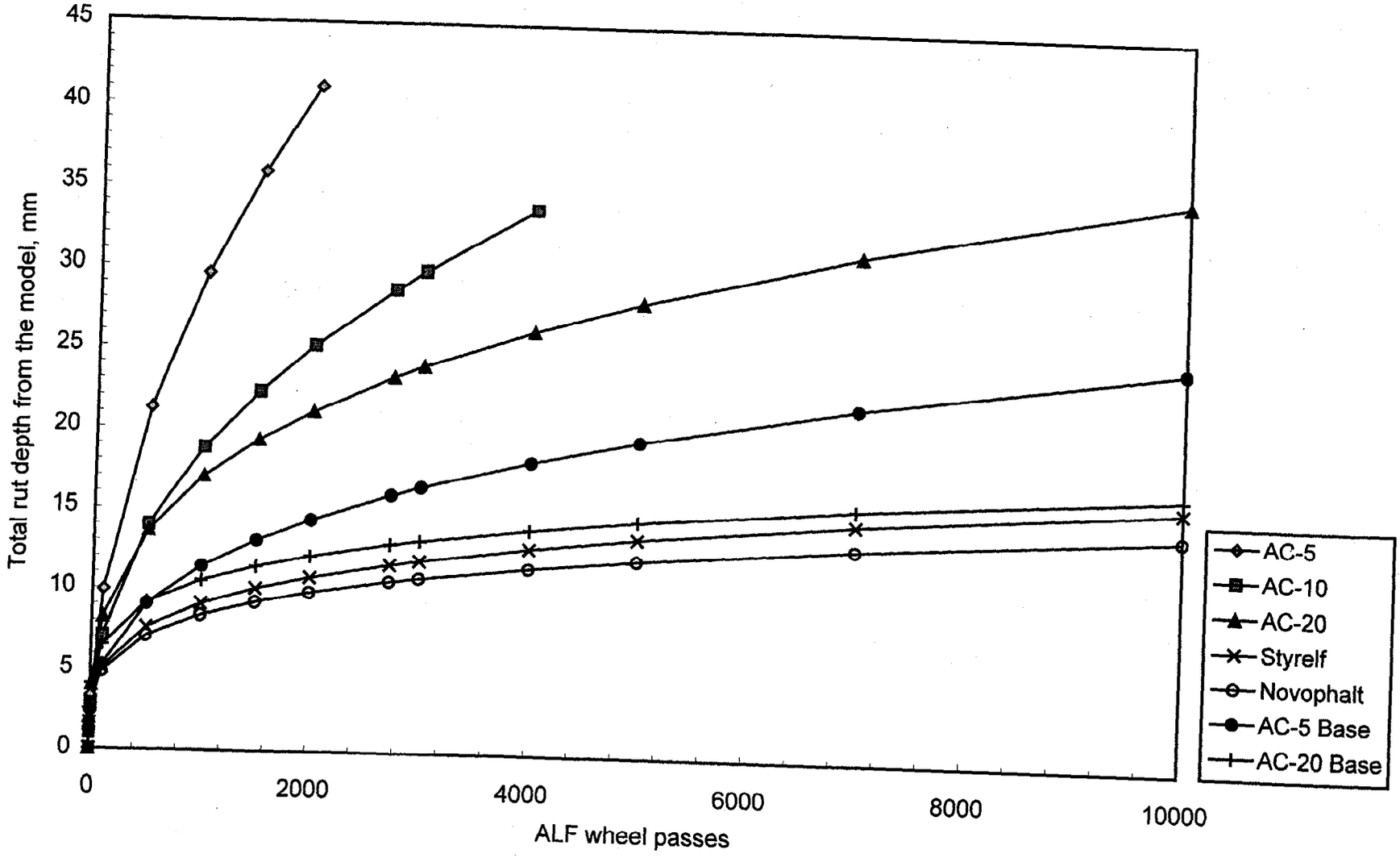

Figure 13. Total rut depth from the model vs. ALF wheel passes.

Table 16. Pavement rankings based on the average ALF wheel passes needed to obtain rut depths of 15 and 20 mm using the raw data and the rut depth model.

Mixture	Temp °C	ALF Wheel Passes at a 15-mm Rut Depth in the Asphalt Pavement Layer		ALF Wheel Passes at a 20-mm Rut Depth in the Asphalt Pavement Layer	
		Raw Data	Rut Depth Model	Raw Data	Rut Depth Model
Novophalt	58	ND[1]	1,750,000[2]	ND[1]	6,000,000[2]
Styrelf	58	32,610	55,540	400,000[3]	220,000[3]
AC-20 Base	58	8,750	11,220	43,780	57,520
AC-5 Base	58	4,170	4,240	10,000	11,990
AC-20	58	1,030	980	2,640	2,730
AC-10	58	1,050	940	1,880	1,900
AC-5	58	480	340	1,410	670

[1]No data; the test was terminated at a rut depth of 9 mm because the mixture stopped rutting.

[2]Determined by extrapolation. The test was terminated at a rut depth of 9 mm (208,805 wheel passes).

[3]Determined by extrapolation. The test was terminated at a rut depth of 18 mm (200,000 wheel passes).

Table 17. Average ALF pavement data.

ALF Wheel Passes Required to Obtain Rut Depths of 10, 15, and 20 mm in the Asphalt Pavement Layer

Mixture	Wheel Passes at a Rut Depth of 10 mm	Wheel Passes at a Rut Depth of 15 mm	Wheel Passes at a Rut Depth of 20 mm
Novophalt	293,000[1]	1,750,000[1]	6,000,000[1]
Styrelf	7,910	55,540	220,000[1]
AC-20 Base	1,120	11,220	57,520
AC-5 Base	990	4,240	11,990
AC-20	230[2]	980	2,730
AC-10	340[2]	940	1,900
AC-5	130	340	670

ALF Wheel Passes Required to Obtain Rut Depths of 10, 15, and 20 mm in All Pavement Layers

Mixture	Wheel Passes at a Rut Depth of 10 mm	Wheel Passes at a Rut Depth of 15 mm	Wheel Passes at a Rut Depth of 20 mm
Novophalt	2,130	11,760	39,600
Styrelf	1,480	7,400	23,200
AC-20 Base	790	5,540	22,100
AC-5 Base	690	2,310	5,450
AC-20	200[2]	710	1,790
AC-10	230[2]	590	1,160
AC-5	110	260	480

Percent Rut Depth in the Asphalt Pavement Layer When the Total Rut Depth is 10, 15, 20, or 30 mm

Mixture	10 mm	15 mm	20 mm	30 mm
Novophalt	33	32	32	31
Styrelf	71	66	63	58
AC-20 Base	94	88	85	79
AC-5 Base	93	86	81	75
AC-20	95	92	89	85
AC-10	84	83	82	81
AC-5	93	90	87	84

[1]Determined by extrapolation.
[2]Reversed ranking compared with the data at 15 and 20 mm.

Table 18. ALF replicate pavement data.

	Surface Mixture AC-5 (PG 59) Lane 9			Surface Mixture AC-20 (PG 70) Lane 10			Base Mixture AC-5 (PG 59) Lane 11		
	Site 2	Site 1	Avg	Site 2	Site 1	Avg	Site 2	Site 1	Avg
Pavement Depth				**Pavement Temperature, °C**					
0 mm	62	61	62	61	59	60	62	58	60
20 mm	59	57	58	59	57	58	60	56	58
102 mm	55	55	55	55	55	55	58	55	56
197 mm	51	52	51	51	51	51	52	50	51
Difference from 0 mm to 197 mm:	11	9	11	10	8	9	10	8	9
	Air Voids, Top 100 mm of Pavement, Percent								
Out of Wheelpath	7.7	7.8	7.8	9.3	8.8	9.1	6.0	7.3	6.7
In Wheelpath	3.6	3.2	3.4	3.4	3.9	3.7	2.2	4.0	3.1
Densification	4.1	4.6	4.4	5.9	4.9	5.4	3.8	3.3	3.6
	Air Voids, Bottom 100 mm of Pavement, Percent								
Out of Wheelpath	7.9	6.1	7.0	9.5	7.2	8.3	6.0	6.1	6.0
In Wheelpath	3.1	2.5	2.8	3.7	3.2	3.4	1.9	2.6	2.2
Densification	4.8	3.6	4.2	5.8	4.0	4.9	4.1	3.5	3.8
Average Decrease for Entire Layer	4.4	4.1	4.3	5.8	4.4	5.2	4.0	3.4	3.7
Rut Depth in Asphalt Layer				**Number of ALF Wheel Passes**					
10 mm	115	143	129	262	206	234	612	1363	988
15 mm	279	395	337	1031	937	984	2946	5544	4245
20 mm	521	814	667	2724	2741	2733	8984	15000	11992
Total Rut Depth				**Number of ALF Wheel Passes**					
10 mm	85	140	112	226	169	197	707	676	692
15 mm	212	310	261	739	687	713	2224	2399	2312
20 mm	407	546	476	1713	1859	1786	5012	5895	5454

Note: Site 2 is listed first because it was tested before site 1.

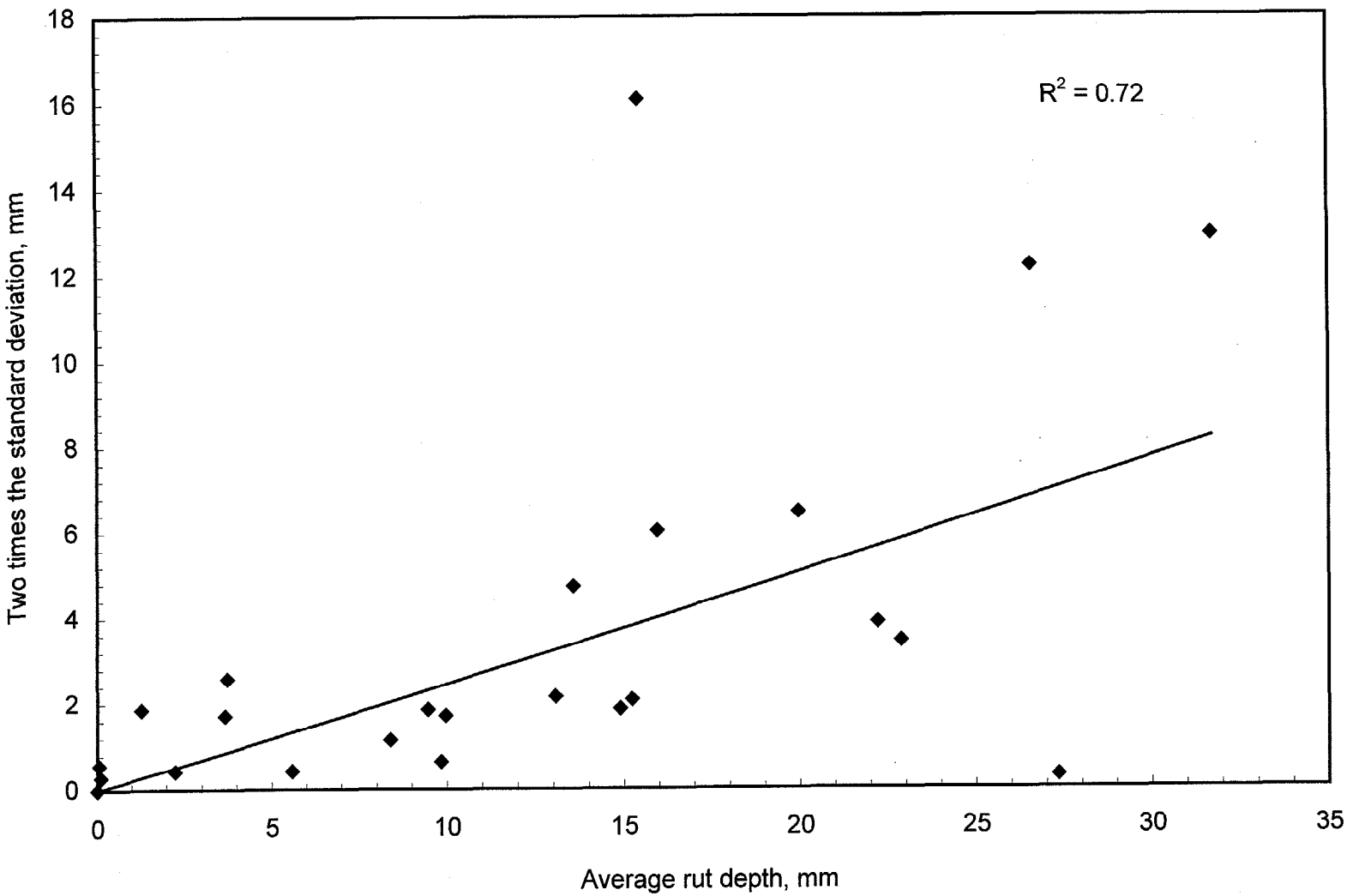

Figure 14. Relationship between two times the standard deviation of the rut depth and the average rut depth.

Table 19. Rankings for the pavements tested at 58 °C based on confidence bands for the rut depth vs. ALF wheel pass relationships.[1]

	Average ALF Wheel Pass at a Rut Depth of 20 mm		Statistical Ranking[2] Based on $\mu \pm 1\sigma_{(n-1)}$		Statistical Ranking[2] Based on $\mu \pm 2\sigma_{(n-1)}$	
	All Mixtures		All Mixtures	Surface Mixtures	All Mixtures	Surface Mixtures
Novophalt	A	6,000,000	A	A	A	A
Styrelf	B	220,000	B	B	B	B
AC-20 Base	C	57,520	B		BC	
AC-5 Base	D	11,990	C		CD	
AC-20	E	2,730	D	C	DE	C
AC-10	F	1,900	D	C	E	C
AC-5	G	670	E	D	F	D

[1]The letters are the statistical ranking, with "A" denoting the mixture with the lowest susceptibility to rutting.

[2]μ = average wheel pass and $\sigma_{(n-1)}$ = sample standard deviation

Table 20. Rankings for the pavements tested at 58 °C based on the coefficient of variation (CV).[1]

	Statistical Ranking Based on Log ALF Wheel Passes at a Rut Depth of 20 mm and a coefficient of variation (CV) of 0.22					
	Average Wheel Pass	Sample Standard Deviation $\sigma_{(n-1)}$	Calculated Replicate Number 1	Calculated Replicate Number 2	Ranking, All Mixtures	Ranking, Surface Mixtures
Novophalt	6,000,000	1,320,000	5,067,000	6,933,000	A	A
Styrelf	220,000	48,400	186,600	255,400	B	B
AC-20 Base	57,520	12,654	48,600	66,400	C	
AC-5 Base	11,990	2,638	10,130	13,860	D	
AC-20	2,730	601	2,310	3,160	E	C
AC-10	1,900	418	1,600	2,200	E	C
AC-5	670	147	560	770	F	D

	Statistical Ranking Based on Log Wheel Passes at a Rut Depth of 10 mm and a CV of 0.29		Statistical Ranking Based on Log Wheel Passes at a Rut Depth of 15 mm and a CV of 0.25	
	All Mixtures	Surface Mixtures	All Mixtures	Surface Mixtures
Novophalt	A	A	A	A
Styrelf	B	B	B	B
AC-20 Base	C		C	
AC-5 Base	C		D	
AC-20	D	C	E	C
AC-10	DE	CD	E	C
AC-5	E	D	F	D

[1]The letters are the statistical ranking, with "A" denoting the mixture with the lowest susceptibility to rutting.

Table 21. Rankings for the five surface mixtures at 58 °C based on G*/sinδ at 2.25 rad/s and ALF pavement performance.

Binder, G*/sinδ at 2.25 rad/s	ALF Pavement Performance
(A) Styrelf	(A) Novophalt
(B) Novophalt	(B) Styrelf
(C) AC-20	(C) AC-20
(D) AC-10	(C) AC-10
(E) AC-5	(D) AC-5

Note: "A" denotes the binder with the highest G*/sinδ or pavement with the lowest susceptibility to rutting.

The rut depths at 2,730 ALF wheel passes were also compared. The AC-20 (PG 70) surface mixture was considered the control mixture in this analysis, and a rut depth of 20 mm was considered the failure level. The rut depths in the AC-20 (PG 70) surface and base mixtures at 2,730 ALF wheel passes were 20 and 12 mm, respectively. The rut depths in the AC-5 (PG 59) surface and base mixtures at 2,730 ALF wheel passes were 35 and 14 mm, respectively. Increased nominal maximum aggregate size and the associated 0.85-percent decrease in optimum binder content significantly decreased rutting susceptibility for both binder grades.

Both analyses showed that the increase in nominal maximum aggregate size from 19.0 to 37.5 mm, and the associated 0.85-percent decrease in optimum binder content, significantly decreased rutting susceptibility based on ALF pavement performance. This was expected. No binder parameter can provide the effects that mixture composition and aggregate properties have on pavement performance. Binder specifications should provide some minimal level of performance.

b. Interaction Between Nominal Maximum Aggregate Size and Grade of Binder

The data in table 17 show that the AC-20 (PG 70) surface mixture required 2,730 wheel passes compared with 670 wheel passes for the AC-5 (PG 59) surface mixture to obtain a rut depth of 20 mm. The wheel passes for the AC-20 (PG 70) surface mixture is 310 percent higher than for the AC-5 (PG 59) surface mixture. The AC-20 (PG 70) base mixture required 57,520 wheel passes compared to 11,990 wheel passes for the AC-5 (PG 59) base mixture. The wheel passes for the AC-20 (PG 70) base mixture is 380 percent higher than for the AC-5 (PG 59) base mixture. At a rut depth of 15 mm, the percent increase in wheel passes obtained by changing from the AC-5 (PG 59) binder to the AC-20 (PG 70) binder was 190 percent for the surface mixtures, and 165 percent for the base mixtures. At a rut depth of 10 mm, the percent increase in wheel passes obtained by changing from the AC-5 (PG 59) binder to the AC-20 (PG 70) binder was 80 percent for the surface mixtures, and 130 percent for the base mixtures. Overall, the percentages for the base mixtures are not significantly lower than the percentages for the surface mixtures. Therefore, the increase in nominal maximum aggregate size and associated 0.85-percent decrease in optimum binder content did not decrease the effect of high-temperature PG on rutting susceptibility on a percentage basis.

6. Evaluation of Other Binder Parameters

a. DSR Parameters From Sine Wave Tests

The following binder parameters were evaluated to determine if they could explain the discrepancy for the Novophalt and Styrelf binders: G^*, δ, $\sin\delta$, $\tan\delta$, δ for RTFO/PAV residues, and $G^*/\sin\delta$ at an angular frequency of 63.1 rad/s. The binder parameters G^*, δ, $\sin\delta$, and $\tan\delta$ were evaluated because of the finding that the Styrelf binder had a lower δ compared with the other binders. Table 22 shows the data for the five binders at frequencies of 10.0 and 2.51 rad/s. An angular frequency of 2.51 rad/s was

used in lieu of the ALF angular frequency of 2.25 rad/s because 2.51 rad/s was the angular frequency closest to 2.25 rad/s at which the DSR automatically recorded data. The data at an angular frequency of 2.25 rad/s would have to be found through interpolation, which was not necessary for this analysis. All data were recorded at a test temperature of 60 °C. Three replicate tests were performed on each binder.

Table 22 shows that all parameters provided the same ranking. All averages for a given parameter were found to be significantly different at a 95-percent confidence level. The ranking for the binders was not dependent on angular frequency.

The phase angles after RTFO/PAV aging were evaluated to determine the effect of increased aging. The data are given in table 23. The phase angles decreased with increased aging, but the binders ranked the same.

$G^*/\sin\delta$ at an angular frequency of 63.1 rad/s was also evaluated. Table 23 shows that the binders ranked the same at all three angular frequencies. The angular frequency of 63.1 rad/s was based on the equation $\omega = 2\pi/t = 62.8$ rad/s using a loading time of 0.1 s. An angular frequency of 63.1 rad/s was used in lieu of 62.8 rad/s because 63.1 rad/s was the angular frequency closest to 62.8 rad/s at which the DSR automatically recorded data.

b. Zero Shear Viscosity

Zero shear viscosity, or low shear rate limiting viscosity, was also measured at 60 °C using the DSR. In this test, the viscosity of a binder is measured at progressively lower shear rates until a constant viscosity is obtained. This viscosity does not include the time dependent recoverable strain when this type of strain exists. Time-dependent recoverable strains are not measured in the Superpave DSR test because it does not include a rest period after each loading cycle. This strain is erroneously included in the permanent strain.

The zero shear viscosities are shown at the bottom of table 22. The ranking provided by this parameter was the same as that provided by the other parameters, and the averages were found to be significantly different at a 95-percent confidence level.

c. Cumulative Permanent Strain After Four Cycles of Repeated Loading

When evaluating asphalt mixtures for rutting susceptibility using repeated load tests, a rest period is generally added after each cycle of loading to simulate how pavements are loaded. At temperatures used in these tests, generally from 0 to 60 °C, the strain vs. time relationships after unloading provide three types of strain: (1) an elastic strain that is instantaneously recovered, (2) a delayed elastic strain that is recovered over time, and (3) a permanent strain that is not recovered. The amount of delayed elastic strain that is recovered increases with an increase in the rest period until

Table 22. Binder parameters at 60 °C after RTFO.

Binder Parameter	AC-5	AC-10	AC-20	Novophalt	Styrelf
G*/sinδ, Pa, 10.0 rad/s	2 096	4 202	7 897	16 580	28 500
G*/sinδ, Pa, 2.51 rad/s	526	1 084	2 100	4 914	11 570
G*, Pa, 10.0 rad/s	2 070	4 133	7 707	15 700	23 600
G*, Pa, 2.51 rad/s	523	1 076	2 075	4 740	9 535
Phase Angle, δ, 10.0 rad/s	81.0	79.6	77.4	71.2	55.9
Phase Angle, δ, 2.51 rad/s	84.2	83.0	81.2	74.7	55.5
sinδ, 10.0 rad/s	0.988	0.984	0.976	0.947	0.828
sinδ, 2.51 rad/s	0.995	0.993	0.988	0.965	0.824
tanδ, 10.0 rad/s	6.31	5.45	4.47	2.94	1.48
tanδ, 2.51 rad/s	9.84	8.14	6.46	3.66	1.46
Zero Shear Viscosity, Pa·s	241	514	1 050	2 960	13 200

Table 23. Additional tests on the five ALF binders at 60 °C.

	RTFO Residue		RTFO/PAV Residue	
	Phase Angle Angular Frequency, rad/s		Phase angle Angular Frequency, rad/s	
Binder	2.51	10.0	2.51	10.0
Novophalt	74.7	71.2	64.7	61.7
Styrelf	55.5	55.9	50.0	50.8
AC-20	81.2	77.4	70.9	67.2
AC-10	83.0	79.6	73.5	69.4
AC-5	84.2	81.0	75.3	70.8

Binder Parameter	AC-5	AC-10	AC-20	Novophalt	Styrelf
G*/sinδ, Pa, 63.1 rad/s	10 455	20 364	36 410	73 155	86 787
G*/sinδ, Pa, 10.0 rad/s	2 096	4 202	7 897	16 580	28 500
G*/sinδ, Pa, 2.51 rad/s	526	1 084	2 100	4 914	11 570

all of this strain is recovered. Virtually no delayed elastic strain is recovered when there is no rest period, as in the DSR test. Thus, if a binder being tested by the DSR has a delayed elastic strain, this strain will be included in the permanent strain. This may lead to a $G^*/\sin\delta$ that is too low compared with the $G^*/\sin\delta$'s of binders that have no delayed elastic strain. It may also be low based on comparisons with pavement performance or the results of repeated load mixture tests that use rest periods. Unmodified asphalt binders generally do not have a significant amount of delayed elastic strain at temperatures used to determine their high-temperature PG.

The five ALF binders were tested using a stress-controlled DSR to determine whether they had measurable delayed elastic strains and, if they did, whether this strain varied from binder to binder and could account for the discrepancy concerning Novophalt and Styrelf. A 500-Pa stress was applied to each binder in the form of a square wave with a load duration of 1.0 s, followed by a rest period. Four cycles of loading and unloading were applied. Rest periods of 1.0 and 9.0 s and test temperatures of 52, 64, and 70 °C were employed. The strain was continuously recorded during the test. Typical stress vs. time and strain vs. time relationships are shown in figure 16.

One method used to evaluate asphalt mixtures for rutting susceptibility consists of measuring the amount of permanent strain that accumulates due to some specified number of loading cycles. The five ALF binders were evaluated in this manner, but only four cycles of loading were used because this was the maximum number of cycles that the DSR could apply. Table 24 shows the cumulative permanent strains after the four cycles of loading. Cumulative permanent strain increased with temperature as expected. The data show that the five binders ranked the same at both rest periods and at all three temperatures. This ranking matched the previous rankings shown in table 22. The data indicated that Styrelf should be least susceptible to rutting.

The percent decrease in cumulative permanent strain due to the use of the longer rest period is included in table 24. Binders that recover more delayed elastic strain during the rest period relative to the total strain will have a greater percent decrease in cumulative permanent strain. Table 24 shows that Styrelf had the highest percent decrease at each temperature, followed by Novophalt. The percent decrease was small for each of the three unmodified binders at all three temperatures. If time dependent recoverable strains were to be taken into account in the binder specification, Styrelf would be the best binder in terms of rutting resistance, and the $G^*/\sin\delta$'s for the Styrelf and Novophalt binders would be further apart compared with the values provided by the current testing protocols.

Analyses of the percent permanent strain provided by individual cycles of loading also showed the effect of rest period. The data for the fourth loading cycle are given in table 25. Binders that recovered more delayed elastic strain during the longer rest period have greater decreases in the percent permanent strain per cycle. Equation (3) in this chapter showed that dissipated energy is proportional to permanent strain. Table 25 shows that the decrease in permanent strain due to the increase in rest period was low

to none for Novophalt and the three unmodified binders at all three temperatures. Therefore, the dissipated energies and PG's for these binders would not be expected to change significantly with the addition of a rest period. The permanent strain at 52 °C for the Styrelf binder using a 9-s rest period was less than half of the permanent strain using a 1-s rest period. In Superpave, each time dissipated energy is halved, the PG increases one grade, or 6 °C. Therefore, it is possible that the use of a 9-s rest period would increase the PG of the Styrelf binder by one grade. The effect of the rest period should decrease with an increase in temperature; therefore, it was hypothesized that the effect of the rest period on the Styrelf binder would be low if it were to be tested at its high-temperature grade of 88 °C. However, the data show that when testing binders at the same temperature, there can be an error in $G^*/\sin\delta$ if a rest period is needed but not used. Even so, the use of a rest period in this study would make the $G^*/\sin\delta$'s for Styrelf and Novophalt be further apart. Thus, the discrepancy was not related to the absence of a rest period.

The percent permanent strains per loading cycle are relatively high in table 25 compared with the percent permanent strains from repeated load mixture and pavement tests. For example, the percent permanent strain per ALF wheel pass at 58 °C was estimated to range from 0.6 percent for the Novophalt surface mixture to 2.9 percent for the AC-5 (PG 59) surface mixture. Table 25 shows that the percent permanent strain per loading cycle in the DSR test would be above 80 percent at 58 °C for all binders except Styrelf. Aggregate interlock is a major factor affecting the results of mixture and pavement tests. Because of these large differences in strain, any interaction between the effects of the binders and the aggregate may lead to discrepancies in the rankings provided by binder and mixture tests. The Superpave binder specification does not consider interactions. Appendix D provides additional data.

7. Properties of Binders Recovered From Pavement Cores

Binders were extracted and recovered from cores and tested by the DSR after the ALF pavement tests were completed. Whether the Novophalt binder could be recovered without the properties of the binder being altered by the heat and solvent used in the process was questionable. Advanced Asphalt Technologies, which supplied the binder, performed tests that indicated it could be recovered using a rotary evaporator. An additional test was performed by the Federal Highway Administration (FHWA) to confirm Advanced Asphalt Technologies' finding. Samples of the Novophalt binder were aged using the RTFO and then tested by the DSR before and after recovery. The binder samples were soaked in solvent before recovery for the length of time the binder would be in solvent if it were to be extracted from aggregates. The binder samples were not mixed with aggregates, and it was assumed that no polyethylene would get caught in the filter during an actual extraction. The recovery process did not affect the average high-temperature continuous PG, being 75.5 °C before recovery and 76.0 °C after recovery. However, none of the recovered binder properties should be assumed to exactly represent in-place binder properties, especially for the two modified binders where the

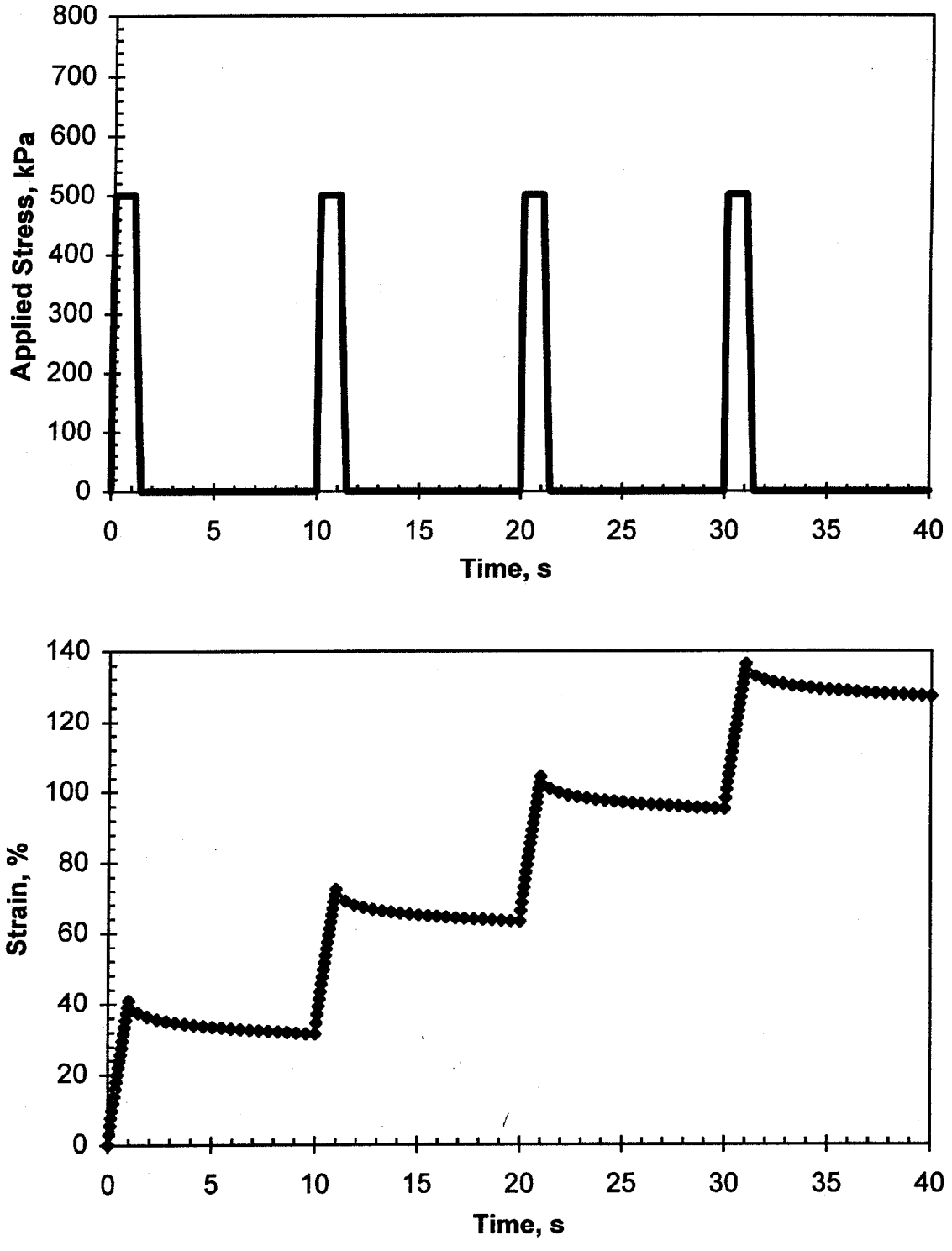

Figure 16. Typical plot of applied DSR stress and resultant shear strain vs. time for the test consisting of a 1.0-s load duration followed by a 9.0-s rest period.

Table 24. Cumulative permanent strain after four cycles of repeated loading using RTFO residues.

Binder	Temperature = 52 °C				Temperature = 64 °C			
	Rest Period			Percent	Rest Period			Percent
	1 s	9 s	Decrease	Decrease	1 s	9 s	Decrease	Decrease
Styrelf	0.07	0.02	0.05	250	0.32	0.15	0.17	88
Novophalt	0.14	0.11	0.03	27	0.84	0.70	0.14	20
AC-20	0.39	0.36	0.03	8	2.91	2.77	0.14	5
AC-10	1.34	1.25	0.09	7	9.73	9.46	0.27	3
AC-5	1.80	1.75	0.05	3	11.40	11.00	0.40	4

Binder	Temperature = 70 °C			
	Rest Period			Percent
	1 s	9 s	Decrease	Decrease
Styrelf	0.63	0.33	0.30	91
Novophalt	1.78	1.49	0.29	19
AC-20	7.03	6.81	0.22	3
AC-10	19.20	18.90	0.30	2
AC-5	24.70	24.30	0.40	2

Table 25. Percent permanent strain for the 4th cycle of loading (Permanent Strain x 100 ÷ Total Strain).

Binder	Temperature = 52 °C			Temperature = 64 °C			Temperature = 70 °C		
	Rest Period			Rest Period			Rest Period		
	1 s	9 s	Decrease	1 s	9 s	Decrease	1 s	9 s	Decrease
Styrelf	72	34	38	77	50	27	79	56	23
Novophalt	89	80	9	94	87	7	95	89	6
AC-20	94	91	3	98	96	2	99	98	1
AC-10	96	92	4	99	99	0	100	100	0
AC-5	97	95	2	99	99	0	100	100	0

Table 26. Properties of binders recovered from cores taken from the wheelpath after performing the ALF pavement test for rutting.

Mixture Type	High-temperature continuous PG based on a G*/sinδ of 2.20 kPa and an angular frequency of 10.0 rad/s			G*/sinδ at 10.0 rad/s and the pavement test temperature of 58 °C	
	RTFO Residue	Recovered Binder, 1994 Test	Recovered Binder, 1995 Test	Recovered Binder, 1994 Test	Recovered Binder, 1995 Test
AC-5 Surface and Base Mixtures					
AC-5 Surf	59	63	68	4.3	7.9
AC-5 Base	59	67	72	6.9	12.7
AC-20 Surface and Base Mixtures					
AC-20 Surf	70	72	78	12.4	25.0
AC-20 Base	70	78	NT	29.0	NT
Other Surface Mixtures					
AC-10	65	67	NT	7.2	NT
Novophalt	77	81	NT	29.1	NT
Styrelf	88	86	NT	37.3	NT

NT = Not tested.

structure of the two-phase system may depend on time and aggregate surface properties.

The high-temperature continuous PG's of the binders are shown in table 26. The binders recovered from the 1994 pavement cores were stiffer than the RTFO residues, except for the Styrelf binder. The greatest difference in temperature for the five surface mixtures was 4 °C, which was provided by the Novophalt binder (81 versus 77). This difference was relatively small compared with the difference of 8 °C provided by the two base mixtures: 67 versus 59 for the AC-5 (PG 59) base mixture, and 78 versus 70 for the AC-20 (PG 70) base mixture. Most likely, the 0.85-percent lower binder content for the base mixtures allowed more aging to occur during construction and early pavement life.

The 1994 core data in table 26 show that the AC-5 (PG 59) base mixture was 4 °C higher in grade than the AC-5 (PG 59) surface mixture (67 versus 63). The AC-20 base mixture was 6 °C higher in grade than the AC-20 (PG 70) surface mixture (78 versus 72). These differences may be an additional reason why each base mixture performed significantly better than its associated surface mixture when tested by the ALF. The G*/sinδ's at 10.0 rad/s and 58 °C also show the differences in binder properties.

Although the three pavements tested in 1995 were considered replicate pavement tests, the 1994 and 1995 PG's suggest that the pavements had aged between 1994 and 1995. Table 18 shows that the numbers of ALF wheel passes needed to obtain rut depths of 10, 15, and 20 mm in the asphalt pavement layer were higher in 1995 (site 1) compared with 1994 (site 2) for the AC-5 (PG 59) surface and base mixtures. These increases in wheel passes could be due to age hardening. The 1995 and 1994 wheel passes (sites 1 and 2) for the AC-20 (PG 70) surface mixture were virtually equal, thus age hardening appeared to have little to no effect on the pavement performances of this mixture. If age hardening was a factor in this study, its effect was that it increased the standard deviation used to rank the mixtures in tables 19 and 20, thus making it more difficult for the ALF pavement performances of the mixtures to be significantly different.

The 1994 core data did not explain the reversal in performance for the Novophalt and Styrelf binders. The PG's for the recovered binders show that the Styrelf binder had a higher grade than the Novophalt binder, although the difference in PG was only 5 °C (86 versus 81) compared with 11 °C (88 versus 77) for the RTFO residues.

8. Conclusions

- In general, binders with higher G*/sinδ's after RTFO aging provided mixtures with lower pavement rutting susceptibilities for a given nominal maximum aggregate size.

- The main discrepancy between G*/sinδ at 58 °C after RTFO aging and the ALF pavement performances of the five surface mixtures at 58 °C

was that the Novophalt binder had a G*/sinδ of 6.83 kPa compared with 13.7 kPa for the Styrelf binder, but the asphalt pavement layer with Novophalt had a significantly lower susceptibility to rutting. The

ALF produced a rut depth of 20 mm in the asphalt pavement layer with Styrelf at 220,000 wheel passes. The rut depth in the asphalt pavement layer with Novophalt was only 9.4 mm at 220,000 wheel passes.

- The following binder parameters did not explain the discrepancy provided by the Novophalt and Styrelf binders: G*, δ, sinδ, tanδ, zero shear viscosity, δ using RTFO/PAV residues, G*/sinδ after RTFO at angular frequencies ranging from 2.51 to 63.1 rad/s, cumulative permanent strain after four cycles of repeated loading, and G*/sinδ of binders recovered from pavement cores. All binder properties ranked Styrelf higher than Novophalt.

- The increase in nominal maximum aggregate size from 19.0 to 37.5 mm, and the associated 0.85-percent decrease in optimum binder content, decreased rutting susceptibility based on ALF pavement performance. To obtain a rut depth of 20 mm in the asphalt pavement layer, the AC-5 (PG 59) base mixture required 11,990 wheel passes compared with 670 wheel passes for the AC-5 (PG 59) surface mixture. The AC-20 (PG 70) base mixture required 57,520 wheel passes compared with 2,730 wheel passes for the AC-20 (PG 70) surface mixture. The effect was statistically significant for both binder grades.

- Part of the decrease in pavement rutting susceptibility provided by the increase in nominal maximum aggregate size could have been due to differences in age hardening. The high-temperature continuous PG of the binder recovered from the AC-5 (PG 59) base mixture was higher than the high-temperature continuous PG of the binder recovered from the AC-5 (PG 59) surface mixture. The same result was found for the two mixtures containing the AC-20 (PG 70) binder. Most likely, the 0.85-percent lower binder content for the base mixtures allowed more aging to occur during construction and early pavement life.

- Although the increase in nominal maximum aggregate size decreased rutting susceptibility, it did not reduce the influence of binder grade on rutting performance on a percentage basis. The increase in ALF wheel passes resulting from an increase in the high-temperature continuous PG from 59 to 70 was 310 percent for the surface mixtures and 380 percent for the base mixtures.

9. Comment on Binder Specifications

- No binder parameter can provide the effects that mixture composition and aggregate properties have on pavement performance, including the effect of nominal maximum aggregate size and changes in binder content. Binder specifications should provide some minimal level of performance.